Potential impact of surface microstructure change on reduction of emission current in tungsten filament

Fusion Engineering and Design 199 (2024) 114144

Contents lists available at ScienceDirect

Fusion Engineering and Design

journal homepage: www.elsevier.com/locate/fusengdes

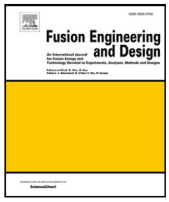

Potential impact of surface microstructure change on reduction of emission current in tungsten filament

Ryuichi Sakamoto *, Kenichi Nagaoka, Daisuke Nagata, Yutaka Fujiwara[1], Mamoru Sato, Katsuyoshi Tsumori

National Institute for Fusion Science, Oroshi 322-6, Toki, 509-5292, Gifu, Japan

ARTICLE INFO

Keywords:
Neutral beam injection
Helium beam
Helium irradiation
Micro surface structure

ABSTRACT

When a helium beam is extracted, a significant decrease in arc current is observed in the filament arc ion source of the Neutral Beam Injector. Microstructural changes in the tungsten filament surface of the ion source are observed by electron microscopy to investigate the cause of the reduction of arc current. Helium bubbles with 100–800 nm diameters appear immediately beneath the surface within 1 μm, and the bubbles develop into surface hole structures with surface erosion by sputtering. The decrease in arc current with helium beam extraction can be explained by a reduced effective surface area, due to the increase in hole porosity. It has been shown that the reduction of the arc current can be recovered by removing the helium-irradiation-affected layer by sputtering with argon discharge.

1. Introduction

Plasma heating by α particles (high-energy helium particles) produced by a D-T fusion reaction and rapid helium exhaust after transferring energy to plasma, these helium behaviors have significance in establishing a fusion reactor. High-energy helium beam injection experiments have been performed by changing the working gas of the Neutral Beam Injector (NBI) from hydrogen to helium in the Large Helical Device (LHD) to simulate the helium behavior (transport and exhaust) in the burning plasma of fusion reactors, including ITER and DEMO. In NBI, Hydrogen ions are extracted from the filament arc ion source, electrostatically accelerated, and then neutralized by the charge exchange process by passing through a gas cell to generate a neutral hydrogen beam. However, when the working gas is changed to helium to extract the helium beam, the arc current of the filament arc ion source is drastically reduced, causing a decrease in the helium beam power.

Many studies have been conducted on the impact of helium irradiation on tungsten as a plasma-facing material, and the formation of nanoscale surface damage structures due to helium plasma irradiation is well known. The plasma exposure is characterized by low-energy particle injection with high-particle flux. And therefore, a large number of plasma particles are dynamically implanted immediately beneath the surface within ~ 10 nm. In particular, due to the strong interaction of helium with vacancies [1,2], helium nanobubbles are formed, and helium is stably trapped in the bubbles, even at high temperatures. It has also been shown that nanoscale hole structures are formed in association with the formation of helium bubbles [3–5]. In analogy with these previous studies, we hypothesized that the decrease in arc current was caused by changes in the surface structures of tungsten filament due to the helium irradiation effect, and microstructural observation with electron microscopies has been applied to investigate the helium effect on the tungsten filament.

Furthermore, to recover the surface structural change of the filament caused by helium irradiation, we attempted to remove the surface layer by sputtering with argon discharge. As discussed in [1], rare gases generally strongly interact with vacancies, and there are concerns that argon irradiation may have similar effects to helium irradiation. Due to its larger mass than helium, argon has a shorter range into tungsten, and the sputtering rate is higher than helium. Therefore, erosion is predicted to predominate over a surface-affected layer's formation under argon discharge [6], and an irradiation-affected layer will not be formed as in the case of helium irradiation.

2. Tungsten filament

The filament arc ion source, which is used in the helium beam injection experiment, extracts an arc current by accelerating a thermoelectron from a tungsten hot filament. As shown in Fig. 1(a), the

* Corresponding author.
E-mail address: sakamoto@nifs.ac.jp (R. Sakamoto).
[1] Present address: University of California, Irvine, Department of Physics and Astronomy, USA.

https://doi.org/10.1016/j.fusengdes.2023.114144
Received 25 August 2023; Received in revised form 9 December 2023; Accepted 31 December 2023
Available online 4 January 2024

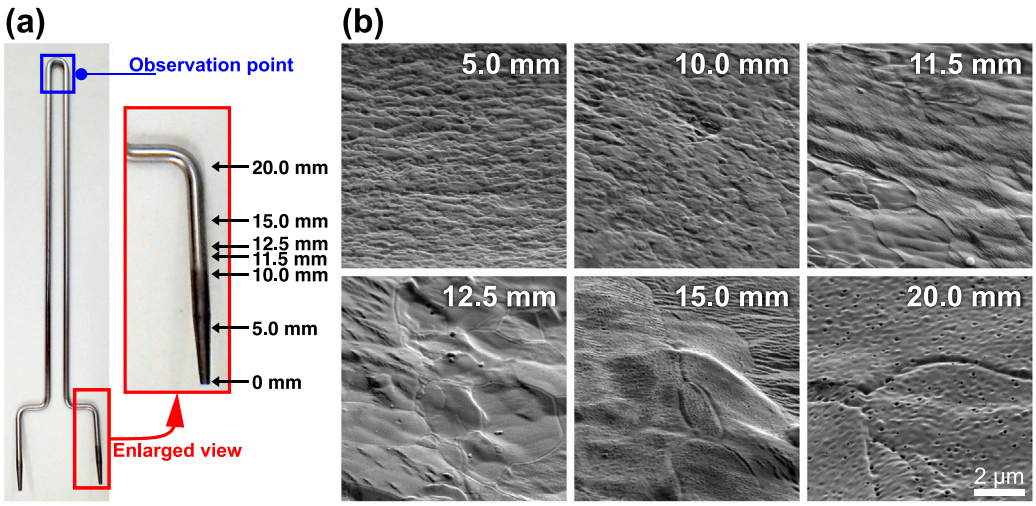

Fig. 1. Tungsten filament of the arc ion source of NBI. (a) Overview image of the filament. The red square shows the terminal area connecting to water-cooled copper electrodes. The terminal area remains unaffected by the high temperature and plasma exposure and retains the original surface structure as sintered tungsten. The blue square shows the representative area to be observed in this study. (b) Surface microstructure variation along the filament at the terminal area (red square).

filament is made of 1.8 mm diameter, 200 mm long pure tungsten wire, and 12 filaments are used in the ion source operation. The typical arc current is about 800 A. In addition to the thermionic emission component from a filament, an ion current component flows into the filament from the arc plasma. Considering plasma density in the ion source, the particle flux to the filament is estimated to be 1.0×10^{22} m^{-2}. This value is comparable to the particle flux at the divertor, showing that the filament is placed in a severe particle load environment.

Tungsten is a candidate material for the divertor target plate in ITER and future fusion reactors, and studies on the plasma irradiation effect of tungsten have been widely conducted [7–9]. On the other hand, the major difference between filament and diverter is the operating temperature. The divertor is used below the recrystallization temperature (~ 1300 K) for preventing mechanical property degradation due to grain growth. In contrast, the filament is used at very high temperatures (~ 2900 K) for maximizing thermionic emission.

Typical filament surface microstructures, which are observed by a Scanning Electron Microscope (SEM), are shown in Fig. 1(b). The filament's end parts, indicated in the red square, are inserted 10 mm into water-cooled copper electrodes, and the temperature is kept moderate. Therefore the SEM images at 5.0 mm and 10.0 mm from the end show the original surface structure as sintered tungsten. The filament temperature increases steeply with distance from the water-cooled electrode, and grain growth starts to be observed at 11.5 mm by recrystallization. The grain size increases as the distance from the water-cooled electrode, and the grain size at 20.0 mm is comparable to one at the tip of the filament, which is indicated in the blue square. We chose the tip of the filament as representative of the filament.

Fig. 2 shows a waveform of ion source operation with helium. The typical pulse width of helium beam extraction is 0.5 s in LHD plasma experiments. A 5 – 10 s pre-arc duration is needed to optimize arc plasma conditions. The arc current decreases from 760 A to 400 A within 4 shots of 0.5 s beam extraction and asymptotically approaches ~ 140 A. The arc current decrease can also be observed during beam extraction. The typical reduction rate in arc current is ~ 32 A/s under the constant voltage control of the arc power supply. During the helium beam extraction, no apparent changes were observed in the operation parameters except for the arc current and beam current. Since these helium beam extractions were operated for the plasma experiments with the working injector, detailed plasma parameters in the ions source could not measured. In the LHD plasma experiments, helium beam operation can be repeated with an arc current of 670 A every 7 shots. 6 shots between helium discharges are argon discharges for recovering the adverse effects of helium discharge.

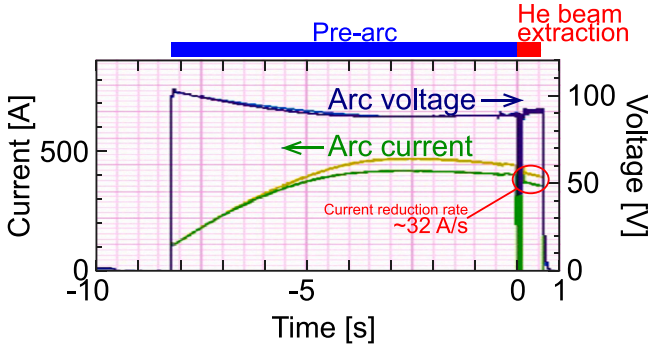

Fig. 2. Figure shows a typical waveform of the operation of the two ion sources with helium. The pulse width of helium beam extraction is typically 0.5 s in LHD plasma experiments. Blue and dark blue lines denote arc voltages, and yellow and green lines denote arc current. The arc currents decrease during helium beam extraction at ~32 A/s.

The filaments observed in this study were taken out from the ion source of the NBI after beam extraction under the following four conditions.

1. Reference (Multiple hydrogen discharges): A filament used for extended periods in hydrogen beam extraction.
2. Sample 1 (Helium discharge): A filament used once in a helium beam injection experiment. The arc current was initially 762 A and then decreased to 320 A.
3. Sample 2 (Multiple helium discharges): A filament used in multiple helium beam extraction until the arc current degradation was saturated. The arc current was initially 762 A and then decreased to 137 A.
4. Sample 3 (Argon recovering discharge after helium discharge): A filament exposed to argon discharge after a helium beam extraction to remove the helium exposure affected layer. The arc current was decreased from 803 A to 400 A with the helium beam extraction, and then the arc current recovered to 670 A after argon discharge.

3. Result

Fig. 3 shows SEM images of each filament surface, (a, A) Multiple hydrogen beam extraction, (b, B) Single helium beam extraction, (c,

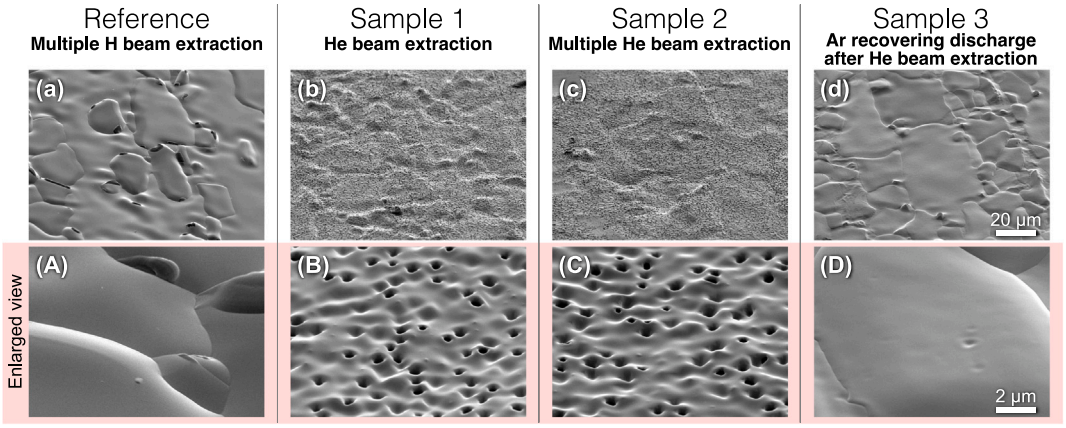

Fig. 3. SEM images of filament surface after beam extraction. (a, A) Reference: Multiple hydrogen beam extraction, (b, B) Sample 1: Single helium beam extraction, (c, C) Sample 2: Multiple helium beam extraction, (d, D) Sample 1: Argon recovering discharge after helium beam extraction.

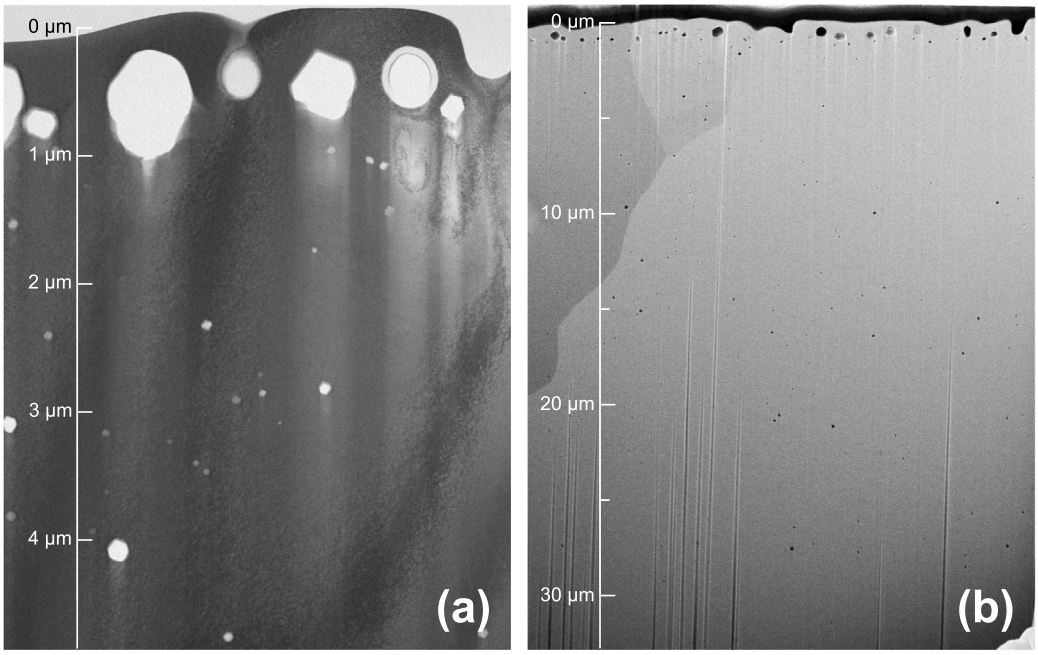

Fig. 4. Cross-sectional (a) TEM, (b) SEM observation of the filament after multiple helium beam extraction. Large bubbles with up to 800 nm diameters are formed within 1 μm depth below the surface, and smaller bubbles with 100 nm diameter are distributed beyond 30 μm in depth. The bubble contrast is the opposite between TEM and SEM images.

C) Multiple helium beam extraction, (d, D) Argon recovering discharge after helium beam extraction.

3.1. Hydrogen beam extraction (reference)

In Fig. 3, the crystal grains grow to several 10 μm in size, due to use under high-temperature conditions exceeding the recrystallization temperature. In some areas, secondary crystallization has resulted in large grain boundary-free areas.

The surface contamination, which is recognized as a black contrast, is observed on the edge of the grain. Energy Dispersive X-ray Spectroscopy (EDS) analysis shows that the surface contamination consists of tungsten and oxygen with a ratio of 1:3, possibly indicating the formation of WO_3. Electron diffraction analysis suggests that the contamination has a polycrystalline or amorphous structure.

3.2. Helium beam extraction (sample 1)

Once a filament is used in the helium beam extraction, the arc current rapidly decreases by half, showing a drastic change in thermionic emission in the filament. Microstructural observation with the SEM has been applied to investigate the helium effect on the tungsten filament. Fig. 3(b) shows that the filament surface is covered by infinite black dots. The formation of the black dots obscures the grain boundaries, but the grain grows to several 10 μm in the same manner as the hydrogen beam extraction.

The enlarged view in Fig. 3 (B) clearly shows that the black dot has a hole structure of several 100 nm in diameter, and unevenness with a similar scale (several 100 nm) is formed on the surface. This is similar to the hole structure formed by helium plasma irradiation below 1000 K [4], although the hole size is several 10 nm in the low-temperature range.

It is known that a fuzz nanostructure is formed under helium plasma exposure at a temperature range of 1000 – 2000 K [10]. Since the fuzz nanostructure was not observed on the filament surface, it is predicted that the filament was used at temperatures above 2000 K. This is consistent with the expected operating temperature of tungsten filaments of ~ 2900 K.

3.3. Multiple He beam extraction (sample 2)

As shown in Fig. 3 (c, C), the hole structure of several 100 nm in diameter and unevenness of the surface is observed in the same manner as a helium beam extraction (Sample 1). Compared to the helium beam extraction (Sample 1), the number density of holes is slightly higher, the unevenness is larger, and the grain boundaries are more indistinct.

The filament surface was cut out by a Focused Ion Beam (FIB) to observe the internal structure of the helium-exposed surface. Cross-sectional TEM and SEM images are shown in Fig. 4(a) and (b). Bubbles with diameters of up to 800 nm are formed within 1 μm depth below the surface. And the unevenness, which is equivalent to the bubble size, is also observed. The unevenness of the surface is formed by connecting the bubbles to the surface with the surface erosion, due to sputtering. Immediately after the connection of a bubble to the surface, it is recognized as a hole structure because of its sufficiently deep structure. And then the hole structure gradually becomes shallower due to the progress of surface erosion and redeposition.

It is also important that bubbles smaller than 100 nm in diameter are distributed beyond 30 μm from the surface. Assuming a few 10 eV incident helium energy, TRIM code [11] calculations indicate that the helium implantation depth is less than 10 nm. The formation of bubbles at a depth beyond 30 μm implies very large helium diffusion under filament-specific high-temperature conditions.

3.4. Ar recovering discharge after He beam extraction (sample 3)

As expected, arc current degradation due to a helium beam extraction is recovered by exposing it to argon discharge. As shown in Fig. 3 (d, D), holes and unevenness of the surface disappear by conducting argon discharge and return to the surface condition similar to the hydrogen beam extraction.

A cross-sectional TEM image in Fig. 5 proves the disappearance of the large bubbles and the surface unevenness. However, on the other hand, small bubbles with diameters of 100 nm or less were left behind throughout the whole region, suggesting that it is difficult to completely recover from the effects of helium.

4. Discussion

Microstructural observations of tungsten filaments suggest that the degradation in arc current after helium beam extraction is due to the formation of microstructures in the tungsten filament surface by helium irradiation, i.e., hole structure and surface unevenness.

Thermionic emission from a hot cathode can be expressed in the following equation,

$$\frac{I_s}{S} = AT^2 \exp\left(\frac{-e\phi}{kT}\right) \quad (1)$$

where, I_s, A, T, ϕ, S denote thermionic emission current, the Richardson constant, temperature, work function, and surface area of the hot cathode. We investigate the effect of the change in effective surface area due to the formation of surface structures on thermionic emission. In the hole structure, the effective thermionic emission is expected to decrease because the thermal electrons emitted inside the hole should be reabsorbed, and the potential gradient of the extracting voltage should be weakened inside the hole. Here, the effect of the surface structure is evaluated by the hole porosity. From the images in Fig. 3 (B) and (C), the area of the black contrast is determined as the hole, and its percentage of the surface area is calculated. The hole porosity is 48% for Sample 1 and 62% for Sample 2, while the arc current degradation ratio is 58% and 82% for Samples 1 and 2, respectively. There is a tendency for the arc current to decrease with increasing porosity. On the other hand, the hole porosity change ratio is smaller than the arc current degradation ratio, and the arc current degradation cannot be explained solely by changes in the surface structure.

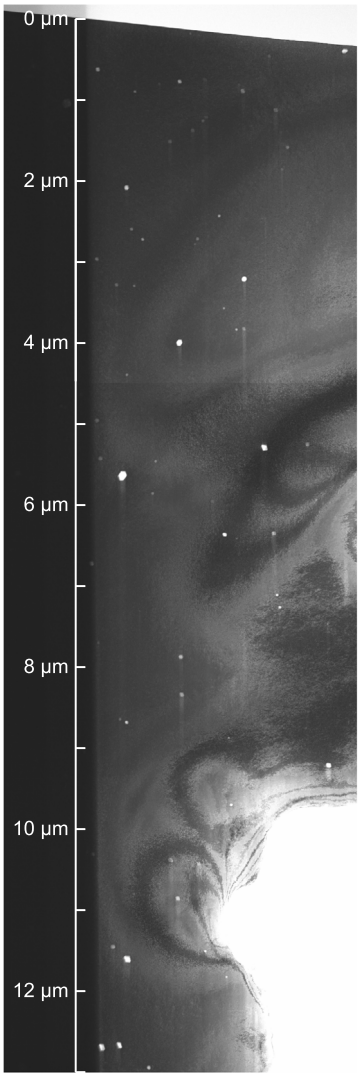

Fig. 5. Cross-sectional TEM observation of the filament with argon recovering discharge after helium beam extraction. Holes and large bubbles at the surface disappear, and surface unevenness is flattened, although tiny bubbles are left behind throughout the whole region. A white region at the bottom of the image is sample damage during the thinning process with FIB.

In Sample 3, the surface structure seems to recover with the argon discharge, as shown in Fig. 3 (D). However, the arc current does not recover to the value before the helium beam extraction, but is still reduced by 17% (800 A to 670 A). Furthermore, the effect of the helium remains inside the filament as a small bubble, as shown in Fig. 5. A possible explanation for the arc current degradation is that the work function may be higher, due to the presence of helium in the tungsten filament. However, our data is insufficient for further discussion of the helium effect on the work function. Further studies on the effect of helium irradiation on the work function are necessary.

5. Conclusion

This work shows that the arc current degradation after helium beam extraction is mainly caused by the change of surface microstructure of the tungsten filament, namely, hole structure formation due to the irradiation effect of helium at high temperatures.

Arc current degradation can be recovered by argon discharge for removing the helium-affected layer by sputtering. On the other hand, the helium influence cannot be completely removed because of extensive

helium diffusion under filament-specific high-temperature conditions. In addition, the arc current will inevitably decrease when the helium beam is extracted again, due to the effects of high-flux helium irradiation. A filamentless RF ion source, which does not depend on the thermionic emission in plasma production, would be an essential solution to these problems.

CRediT authorship contribution statement

Ryuichi Sakamoto: Conceptualization, Investigation, Writing – original draft, Writing – review & editing. **Kenichi Nagaoka:** Investigation. **Daisuke Nagata:** Resources Data curation. **Yutaka Fujiwara:** Investigation. **Mamoru Sato:** Resources Data curation. **Katsuyoshi Tsumori:** Investigation.

Declaration of competing interest

The authors declare that they have no known competing financial interests or personal relationships that could have appeared to influence the work reported in this paper.

Data availability

Data will be made available on request.

Acknowledgments

The authors are grateful to the LHD-NBI group for their experimental support. This work is supported by the National Institute for Fusion Science, Japan grant administrative budgets (NIFS22ULRR702).

References

[1] Atsushi M. Ito, Arimichi Takayama, Yasuhiro Oda, Tomoyuki Tamura, Ryo Kobayashi, Tatsunori Hattori, Shuji Ogata, Noriyasu Ohno, Shin Kajita, Miyuki Yajima, Yasuyuki Noiri, Yoshihide Yoshimoto, Seiki Saito, Shuichi Takamura, Takahiro Murashima, Mitsutaka Miyamoto, Hiroaki Nakamura, Hybrid simulation research on formation mechanism of tungsten nanostructure induced by helium plasma irradiation, J. Nucl. Mater. 463 (2015) 109–115, http://dx.doi.org/10.1016/j.jnucmat.2015.01.018.

[2] Arimichi Takayama, Atsushi M. Ito, Seiki Saito, Noriyasu Ohno, Hiroaki Nakamura, First-principles investigation on trapping of multiple helium atoms within a tungsten monovacancy, Jpn. J. Appl. Phys. 52 (2013) 01AL03, http://dx.doi.org/10.7567/JJAP.52.01AL03.

[3] Dai Nishijima, M.Y. Ye, N. Ohno, S. Takamura, Formation mechanism of bubbles and holes on tungsten surface with low-energy and high-flux helium plasma irradiation in NAGDIS-II, J. Nucl. Mater. 329–333 (Part B) (2004) 1029–1033, http://dx.doi.org/10.1016/j.jnucmat.2004.04.129.

[4] R. Sakamoto, E. Bernard, A. Kreter, N. Yoshida, Surface morphology of tungsten exposed to helium plasma at temperatures below fuzz formation threshold 1073 K, Nuclear Fusion 57 (2016) 016040, http://dx.doi.org/10.1088/1741-4326/57/1/016040.

[5] Mykola Ialovega, Elodie Bernard, Marie-France Barthe, Régis Bisson, Andrea Campos, Martiane Cabié, Thomas Neisius, Ryuichi Sakamoto, Arkadi Kreter, Christian Grisolia, Helium-induced morphology evolution in tungsten under thermal treatment, Nucl. Fusion 62 (2022) 126022, http://dx.doi.org/10.1088/1741-4326/ac94e3.

[6] R.P. Doerner, Sputtering in a high-flux plasma environment, Scripta Mater. 143 (2018) 137–141, http://dx.doi.org/10.1016/j.scriptamat.2017.06.045.

[7] J. Roth, E. Tsitrone, A. Loarte, T. Loarer, G. Counsell, R. Neu, V. Philipps, S. Brezinsek, M. Lehnen, P. Coad, Ch. Grisolia, K. Schmid, K. Krieger, A. Kallenbach, B. Lipschultz, R. Doerner, R. Causey, V. Alimov, W. Shu, O. Ogorodnikova, A. Kirschner, G. Federici, A. Kukushkin, Recent analysis of key plasma wall interactions issues for ITER, J. Nucl. Mater. AL03-391 (2009) 1–9, http://dx.doi.org/10.1016/j.jnucmat.2009.01.037.

[8] Gerald Pintsuk, Akira Hasegawa, Tungsten as a plasma-facing material, in: Comprehensive Nuclear Materials ·, Vol. 6, second ed., 2020, pp. 19–53, http://dx.doi.org/10.1016/B978-0-12-803581-8.11696-0.

[9] Chunyang Luo, Liujie Xu, Le Zong, Huahai Shen Shizhong Wei, Research status of tungsten-based plasma-facing materials: A review, Fusion Eng. Des. 190 (2023) 113487, http://dx.doi.org/10.1016/j.fusengdes.2023.113487.

[10] Shin Kajita, Wataru Sakaguchi, Noriyasu Ohno, Naoaki Yoshida, Tsubasa Saeki, Formation process of tungsten nanostructure by the exposure to helium plasma under fusion relevant plasma conditions, Nucl. Fusion 49 (2009) 095005, http://dx.doi.org/10.1088/0029-5515/49/9/095005.

[11] J.F. Ziegler, J.P. Biersack, M.D. Ziegler, The stopping and range of ions in solids, 2008, https://www.SRIM.org.